UNIVERSITY of York

This is a repository copy of *Thermo-mechanical analysis of hydrogen permeation in lubricated rubbing contacts*.

White Rose Research Online URL for this paper:
https://eprints.whiterose.ac.uk/id/eprint/197009/

Version: Published Version

Article:
Esfahani, Erfan Abedi, Nogorani, Farhad Shahriari and Esfahani, Mohammad Nasr orcid.org/0000-0002-6973-2205 (2023) Thermo-mechanical analysis of hydrogen permeation in lubricated rubbing contacts. Tribology International. 108355. ISSN: 0301-679X

https://doi.org/10.1016/j.triboint.2023.108355

Reuse
This article is distributed under the terms of the Creative Commons Attribution (CC BY) licence. This licence allows you to distribute, remix, tweak, and build upon the work, even commercially, as long as you credit the authors for the original work. More information and the full terms of the licence here: https://creativecommons.org/licenses/

Takedown
If you consider content in White Rose Research Online to be in breach of UK law, please notify us by emailing eprints@whiterose.ac.uk including the URL of the record and the reason for the withdrawal request.

White Rose university consortium
Universities of Leeds, Sheffield & York

eprints@whiterose.ac.uk
https://eprints.whiterose.ac.uk/

Tribology International 182 (2023) 108355

Contents lists available at ScienceDirect

Tribology International

journal homepage: www.elsevier.com/locate/triboint

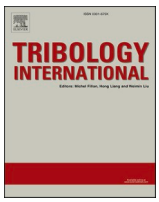

Thermo-mechanical analysis of hydrogen permeation in lubricated rubbing contacts

Erfan Abedi Esfahani [a], Farhad Shahriari Nogorani [b], Mohammad Nasr Esfahani [c,*]

[a] Institute of Functional Surfaces (IFS), University of Leeds, Leeds LS2 9JT, UK
[b] Department of Materials Science and Engineering, Shiraz University of Technology, Shiraz 71557-13876, Iran
[c] School of Physics, Engineering and Technology, University of York, York YO10 5DD, UK

ARTICLE INFO

Keywords:
Hydrogen diffusion
Lubricant degradation, hydrogen embrittlement, molecular dynamics

ABSTRACT

Exploring the fundamental mechanisms of hydrogen generation from a lubricated rubbing contact is a critical step to mitigate premature failure of mechanical elements. This work employs an in-situ hydrogen uptake technique and molecular dynamics simulations to study the thermo-mechanical effects on the hydrogen generation in lubricated contacts. The hydrogen uptake is measured on AISI 52100 bearing steel at temperature of 27 °C and 85 °C under applied pressure of 140 kPa and 350 kPa. Experimental measurements are modeled through atomic simulations using the reactive force field potential. The hydrogen generation associated with the Poly Alpha Olefin decomposition is studied through calculating the pair distribution function. Findings demonstrate enhancing hydrocarbon decomposition with increasing temperature and pressure, while a critical pressure is required for the decomposition process at the ambient temperature. The critical pressure for lubricant degradation is reduced with increasing the temperature. This study highlights the incorporation of thermo-mechanical effects on the hydrogen generation for the design and development of lubricated rubbing contacts.

1. Introduction

Wind energy has been reported as the second source of power production in Europe according to a study conducted by Wind Europe [1]. The majority of rolling element bearings commonly used in wind turbines are made from through hardened and case hardened steels, where the through hardened AISI 52100 steel is widely used in the wind turbine gearboxes in different heat treatment conditions by offering unique mechanical properties [2]. Despite of wide range applications, AISI 52100 alloys are susceptible to "hydrogen embrittlement" leading to a loss of ductility. This premature failure in rolling contact bearings in wind turbines has a direct impact on the energy price due to the downtime and maintenance costs. Various efforts have been carried out to study the hydrogen embrittlement in rolling contact bearings. Uyama et al. [3] and Ciruna et al. [4] report hydrogen content in the bearing steel as one of the major reasons of the reduced bearing life cycles. They found that fatigue life of bearing steel is inversely proportional to the hydrogen content in the steel. For instance, they correlated the reduction of fatigue life of the bearing steel about three orders of magnitude only with the diffusion of 4 ppm hydrogen into the steel. Similarly, Uyama et al. [3] showed that increasing the hydrogen content in the steel, from 0.03 mass-ppm to 1.2 mass-ppm, reduces the fatigue life more than one order of magnitude. Such a shorter life of hydrogen-charged steels is linked to the localised microstructural changes under rolling-contact fatigue (RCF) tests. There are various resources generating atomic hydrogen in lubricated mechanical elements such as lubricant contamination, water in lubricant, tribochemical and thermal lubricant decomposition [3,5,6]. In this respect, frictional heating and shear stress are the other parameters promoting the lubricant decomposition in bearings [7]. The atomic hydrogen in the mechanical components can impose several detrimental impacts leading to a reduction in lifetime through premature failure [4,8]. In tribological components, the hydrogen atoms can be considered as one of the important drivers to develop white etching cracks (WEC) and rolling contact fatigue [4,9–11]. Unlike hydrogen molecules, hydrogen atoms readily diffuse through the metal due to their small size. Various studies suggest the monoatomic hydrogen generation during the surface rubbing of lubricated contacts, which is a direct result of the lubricant decomposition during tribochemical reactions at the contact interface [12]. Therefore, it is important to follow up the hydrogen generation and its permeation rate in order to predict the safe functioning of tribological components. In this respect, Kurten et al. [10] have found no

* Corresponding author.
E-mail address: mohammad.nasresfahani@york.ac.uk (M.N. Esfahani).

https://doi.org/10.1016/j.triboint.2023.108355
Received 29 October 2022; Received in revised form 14 February 2023; Accepted 16 February 2023
Available online 17 February 2023
0301-679X/© 2023 The Author(s). Published by Elsevier Ltd. This is an open access article under the CC BY license (http://creativecommons.org/licenses/by/4.0/).

sign of premature failure in bearings lubricated with a non-hydrocarbon-based lubricant leading to an improvement of the bearing life by preventing the formation of WEC or brittle flaking. This was linked to the lack of hydrogen atoms in the tribochemical decomposition of the lubricant. A similar study on the perfluoropolyether lubricant demonstrates the absence of hydrogen in a lubricated tribo-contact, where no hydrogen permeation was detected during the use of such a hydrogen-free lubricant [13]. Extensive research has been conducted in recent decades to prevent hydrogen-related premature failures by introducing new additives in the lubricant formulations and improving tribological components. Niste et al. [14] reports that WS_2 nanoadditized oil enhances the life cycle of bearing steels through forming a chemical tribofilm on the wear track, which reduces hydrogen ingress into the steel. Several researchers have also found that some sulphur- and phosphorous-containing additives can prevent hydrogen generation from tribo-contacts by deactivating nascent steel surface [7]. In contrast, some anti-wear additives such as zinc dialkyldithophosphate (ZDDP) containing sulphur and phosphorus can promote the hydrogen permeation into the steel by inhibiting the recombination of hydrogen atoms into hydrogen molecules [15]. It is now very well-known that a highly active nascent steel surface accelerates lubricant decomposition leading to a higher hydrogen evolution rate [7]. On the other hand, sulphonates in the lubricant can enhance the hydrogen permeation by hindering the recombination of hydrogen atoms on the surface [16]. In addition to additives in lubricants, surface coating can be used as a tool to mitigate hydrogen diffusion. For example, the use of a diamond-like carbon coating on the steel surface demonstrates a five-fold reduction in the hydrogen desorption from tribochemical lubricant decomposition compared to an un-coated surface [5]. This was traced back to the high gas barrier property of the coating as well as a less friction heat generated at the contact interface of the coated surface.

Experimental results so far have shown that hydrocarbon lubricants are the major source of hydrogen in tribo-contacts [3,5,6,13]. On the other hand, a uniform tribofilm formed across the wear track can act as a physical barrier for hydrogen intrusion and, therefore, reduce hydrogen permeation by impeding the formation of nascent steel surface. Further to those experimental studies, various theoretical approaches have been developed to understand the lubricant behaviour [17,18], hydrogen diffusion [19] and tribochemical reactions [20,21]. Molecular dynamics (MD) is considered as a powerful tool to model oxidation [22] and chemical reactions on the tribological surfaces [20,21].

However, the fundamental mechanisms of hydrogen generation from a lubricated rubbing contact are yet to remain as an ongoing question. In this respect, understanding important factors on the hydrogen generation and its diffusion into the steel are primary steps towards mitigating premature failures of mechanical elements. In this work a combination of computational modeling and experimental results are employed to investigate the complex interplay between operational factors and the hydrogen uptake rate into the steel. A newly developed in-situ measurement technique [13,23] is used to monitor hydrogen intrusion into the steel under various temperature and pressure testing conditions. A reactive MD model is developed to explore experimental measurements through a close replica of the actual tribochemical environment. In the remainder, the sample preparation and measurement technique will be discussed first. This will be followed by describing MD simulations on the hydrogen generation at different temperature and pressure. This work is concluded by a discussion on the thermo-mechanical analysis of hydrogen generation on lubricated contacts.

Table 1
Operating parameters.

Kinematics	Oscillatory motion
Load	35 N and 70 N
Angular displacement amplitude	55 deg.
Temperature	27°C and 85°C
Frequency	1 Hz

2. Materials and methods

2.1. Sample preparation and materials

The metal membrane was made of AISI 52100 bearing steel (containing 1 wt% C and 1.5 wt% Cr). The membrane with a thickness of 800 μm was prepared from a 40 mm diameter bar using a wire cutting machine, where both sides were polished up to 1000 grit SiC grinder paper. One side of the membrane was then coated with a 40 nm of palladium layer to be used as the detection side of the sample where the hydrogen atoms emerge. A K650X sputter coater was utilized to deposit the palladium film. Palladium film was utilized to catalyse atomic hydrogen oxidation and increase the detection efficiency of the measurement [24,25].

The rubbing counterpart was a ring made of 303 stainless steels (Fe-0.1–18 Cr-9Ni-2Mn-1Si-1Cu in wt%) with a contact area of 216 mm^2. Stainless steel was used to minimize the effect of rubbing counterpart corrosion on the hydrogen permeation results, especially in the presence of water contamination in the lubricant. The running surface of the ring was machined to a roughness of Ra ≈ 12 μm. The rubbing interface is comprised of two flat surfaces, which makes the rubbing contact different from most common tribological contacts. Hence, estimation of the lambda ratio is unreliable for such a rubbing contact. The very high roughness of the surface was intentionally employed in order to promote boundary lubrication regime and increase the wear. The high wear volume and large contact area together increase the hydrogen generation rate. Highly pure Poly Alpha Olefin (PAO) synthetic base oil with a kinematic viscosity of about 4.0 cSt at 100 °C was used as the lubricant. No lubricant additives were mixed with the base oil to allow the numerical modeling to investigate basic mechanism of the hydrogen uptake.

2.2. Hydrogen uptake measurement technique

Previous studies reporting hydrogen-induced failures in lubricated surfaces have mainly used ex-situ techniques to measure hydrogen entry into the steel. A newly measurement technique has already been developed to quantify hydrogen permeation in real-time. This novel apparatus enables quantitative measurement of hydrogen permeation from a lubricated contact. This method was employed to study the effect of water contamination, anti-wear and friction modifier additives on tribologically-induced hydrogen uptake from a lubricated interface [13,23].

This setup comprises of a lubricated rubbing part to generate hydrogen and a three-electrode electro chemical cell to detect emerging hydrogen permeated through a thin metal membrane separating the two parts. Hydrogen is produced at the interface of the contact between the steel membrane and a rubbing counterpart. Some of these hydrogen atoms diffuse into the metal membrane and the rest form hydrogen molecules and escape from the surface. Details of this measurement technique can be found in [23].

In this study, the electrochemical detection cell consists of a platinum counter electrode in combination with an Ag/AgCl (3 M KCl) reference electrode, while the steel membrane is used as the working electrode. A compactstat Ivium potentiostat was utilised to apply a constant 115 mV polarization (versus Ag/AgCl electrode) in deaerated 0.1 Molar NaOH solution. This polarised surface will oxidize the hydrogen atoms emerging on the output face. The hydrogen charge can be induced during the manufacturing, heat treatment and preparation processes. Hence, this polarised surface will oxidise the hydrogen atoms emerging on the output surface. Therefore, before rubbing the surface, the metal sample was left until the background current density reached below 250 nA/cm^2. This background current is small enough to show any hydrogen diffusion during the rubbing process. Subsequently, 125

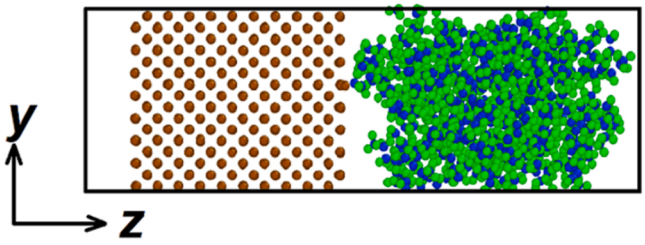

Fig. 1. Initial configuration of iron slab and PAO molecules. The brown, blue and green spheres represent Fe, C and H atoms, respectively.

ml of PAO hydrocarbon base oil lubricant was added to the oil bath, where the rubbing occurs between the surface of the metal membrane and the rubbing counterpart.

In order to contribute to the understanding of the role of contact pressure and temperature on hydrogen permeation rate, tests were conducted at two different loads and two different temperatures as presented in Table 1. The oil circulated through a heat exchanger during the experiment in order to keep the temperature constant. The lubricant flow rate was measured around 25 ml/min. Oscillation occurs between the tribological side of the membrane and the counterpart. Applying the load and starting oscillatory motion only started after the temperature reached the considered level. Once the rubbing started, the oxidation current is captured every 10 s. The hydrogen permeation transient curve and its key features were described previously [13]. Mathematical analysis derived from the Fick's second law can be used to calculate total amount of hydrogen permeation into the steel [23]. Each experiment was repeated at least twice, where the permeation current density was calculated using the average over a longer period of time in the plateau region. The employed in-situ technique has ± 10% repeatability for the recorded values in the plateau region of the curves for an identical measurement condition [13,23]. The steel membrane was unmounted and rinsed with heptane after the test and kept in a desiccator for post-mortem analysis.

2.3. Surface analysis

Raman spectroscopy was employed to chemically characterise the wear scar and achieve a better understanding of the hydrogen permeation mechanism. A Renishaw InVia spectrometer (UK) was employed for Raman spectroscopy analyses with 488 nm wavelength laser operating at a maximum laser power of 10 mW at the source. The laser spot diameter was 800 nm. All Raman spectra were acquired within the range of 150–1670 cm^{-1} at room temperature.

3. Computational models

The reaction between PAO and steel is modeled through using the reactive force field (ReaxFF) potential. This potential considers the chemical reactions, dissociation and formation of chemical bonds, and diffusion, where the energy of the system is written as.

$$E_{sys} = E_{bond} + E_{over} + E_{under} + E_{val} + E_{tor} + E_{pen} + E_{conj} + E_{vdwalls} + E_{coulomb} \quad (1)$$

where E_{bond} is bond energy, E_{over} and E_{under} are the over-coordination and under-coordination energy, respectively, E_{val} is valence angle energy, E_{tor} is the energy associated with torsion angle term, E_{pen} is the penalty energy of over/under coordination in central atom, E_{conj} is the energy of conjunction effects, $E_{vdWalls}$ is the nonbonded van der Waals interactions and E_{colomb} is the nonbond associated with Coulomb energies. This study uses the force field parameters to model lubricant/iron interactions obtained from Aryanpour et al. [26]. An iron slab interfaced with PAO molecules is modeled with applying periodic boundary condition along x - and y-directions, while a fixed boundary condition is considered along z - direction with a reflecting wall at the end of the simulation cell to confine the PAO molecules (Fig. 1). The vacuum slab along z -direction is adjusted such a way to control the pressure in the PAO molecules. Similar approach has been utilised to model oxidation processes [27]. All MD simulations are carried out using LAMMPS frameworks [28]. A Maxwell-Boltzmann distribution is considered for the initial velocities. At first, energy minimisation is performed by a conjugate gradient method to eliminate thermal fluctuations. Then, a canonical (NVT) ensemble is employed using Nose-Hoover thermostats at a temperature of 27 °C. A time step of 0.05 fs is considered for all simulations. The atomic charges are updated for every time step to minimise the electrostatic energy.

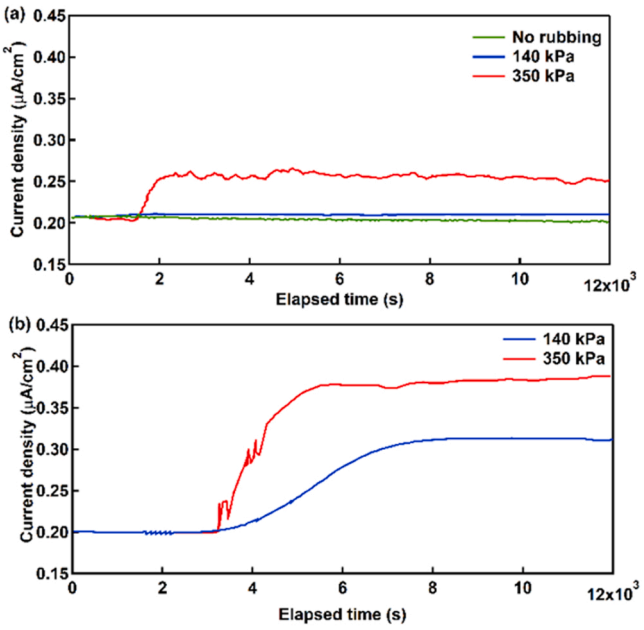

Fig. 2. Current density changes over time at temperature of (a) 27 °C and (b) 85 °C in different pressure levels of 140 kPa and 350 kPa.

4. Results

4.1. Experimental results

In order to understand the influence of contact pressure on hydrogen uptake, experiment was conducted at two different applied loads of 70 N and 35 N, having PAO base oil as lubricant. Considering the contact surface area between the membrane and tribo-couple, the equivalent nominal apparent pressure related to 70 N and 35 N were almost 350 kPa and 140 kPa, respectively. The real pressure at asperity-asperity contacts is much higher especially due to a very rough surface of the counterpart. Fig. 2 demonstrates the current density for different pressure and temperature levels compared with the static system without any rubbing at the ambient condition. At the ambient temperature, the current density is negligible for pressure less than 140 kPa. Three stages are recognised in the measured current density with increasing the pressure and temperature. The first stage is the time that the current density remains in a background level as a latent time. Then there is a significant increase in the current density at the second stage representing a transient situation. In the last stage, the current density reaches to a steady-state condition without any significant changes. In a preliminary analysis, results indicate no hydrogen permeation into the steel for the ambient condition without rubbing. At a temperature of 27 °C, the hydrogen permeation rate is negligible in a pressure of 140 kPa, while the current density changes from 0.2 μA/cm^2 to 0.26 μA/cm^2 after 2000 s in a pressure of 350 kPa. Hydrogen permeation rate raises

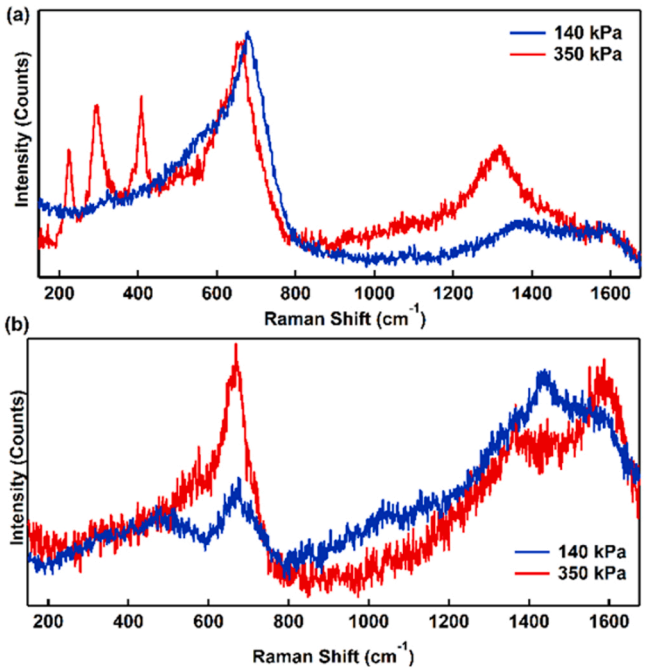

Fig. 3. Raman spectra obtained from wear scars on tribopair after the test using PAO base oil at temperature of (a) 27 °C and (b) 85 °C in different pressure levels of 140 kPa and 350 kPa.

significantly by changing the temperature into 85 °C, while the latent time increases to about 5000 s. The current density changes from the background level to 0.31 μA/cm2 and 0.38 μA/cm2 for a pressure of 140 kPa and 350 kPa at the transient stage, respectively. The transient time for hydrogen atoms to emerge on the detection cell depends on the thickness of the membrane and the metallurgical state of the metal. The steady state current values depend on the hydrogen concentration on the rubbing interface, the membrane thickness and the effective diffusion coefficient. Considering the same membrane thickness and metallurgical state, results in Fig. 2 exhibit changes in the hydrogen concentration on the rubbing interface with increasing temperature and pressure. The change of temperature and frictional heat could affect hydrogen diffusion coefficient of the membrane which assumed to be trivial in this measurement technique. While computational modeling confirms these experimental results, further studies are required to investigate the effect of other parameters, especially due to the complex nature of the lubricated rubbing interface.

After measuring the hydrogen permeation at different temperature and pressure levels, the surface analysis was carried out on the membranes by Raman spectrometry. Fig. 3 presents Raman spectra obtained from wear track of the steel surface after testing with PAO base oil. Raman spectra in Fig. 3(a) exhibit the formation of both hematite (Fe_2O_3) and magnetite (Fe_3O_4) on the surface of the sample tested at the contact pressure of 350 kPa. The formation of hematite is evident from peaks observed between 200 $cm^{-1}$to 400 cm^{-1}, while the Raman peak at 670 cm^{-1}indicates the formation of magnetite. A single Raman peak at 670 cm^{-1} for magnetite is observed within the worn region of the specimen tested at 140 kPa contact pressure [29]. The broad peaks observed at 1370 cm^{-1} and 1590 cm^{-1} belong to the amorphous carbon [30]. On the other hand, Fig. 3(b) reveals magnetite and amorphous carbon formation on both sample surfaces tested at 85 °C at different contact pressures, 140 kPa and 350 kPa. Raman spectra in Fig. 3 show that the magnetite formation is promoted with increasing energy input into the contact by higher load or temperature.

4.2. Computational results

To model the experiments discussed earlier, the reaction between PAO and iron is studied first. Fig. 4 demonstrates the reactive atomic simulations of the iron-PAO system at 27 °C and pressure of 100 kPa over the time. The reaction begins at the early stage of contact PAO with the surface of iron, which can be observed from the chemical interactions between hydrogen and iron (Fig. 4(d)). The hydrogen generation in this reaction includes hydrogen atoms on the iron surface and hydrogen molecules inside PAO. Some of the hydrogen atoms generated on the surface diffuse into the iron slab. This hydrogen generation in lubricated contact is a function of thermal and mechanical boundary conditions. The hydrogen atom diffused into the iron slab can be analyzed based on atomic charge in MD simulations.

The charge distribution of iron, hydrogen and carbon atoms along *z* -direction of the simulation domain at 27 °C and different pressure is shown in Fig. 5. The iron atoms are positively charged and indicate two distinct zones: A thin layer (2–4 Å) of iron atoms with a charge less than + 0.2e inside the iron slab (indicated with dashed line in Fig. 5), and a thick layer (6–8 Å) of iron with a charge more than + 0.4e outside of the iron slab. The thin iron layer on the iron-PAO interface is the zone of diffused hydrogen, while the thick iron layer with high positive charge represents iron atoms penetrated into the lubricant through chemical reactions. The hydrogen atoms create three distinct zones. The major

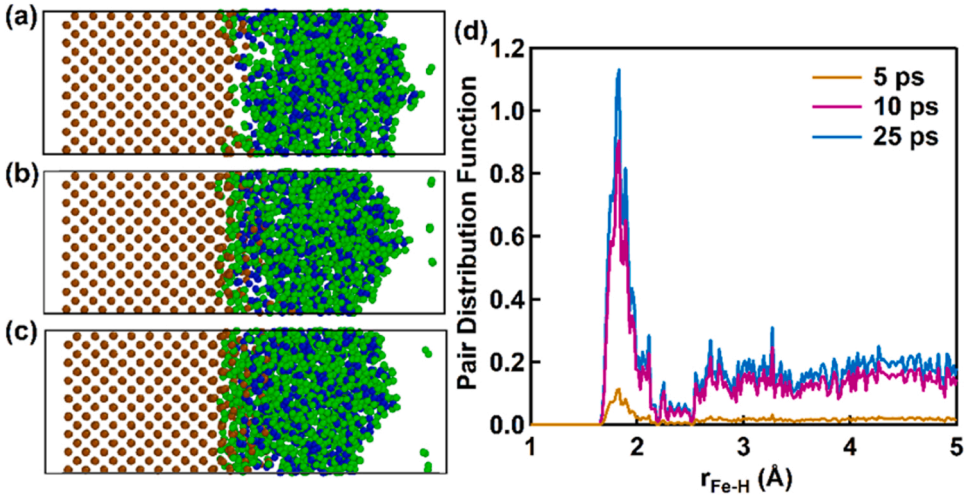

Fig. 4. The proceeding of iron/PAO interactions at 27 °C and pressure of 100 kPa after (a) 5 ps, (b) 10 ps and (c) 25 ps associated with (d) Fe-H pair distribution functions. The brown, blue and green spheres represent iron, carbon and hydrogen atoms, respectively.

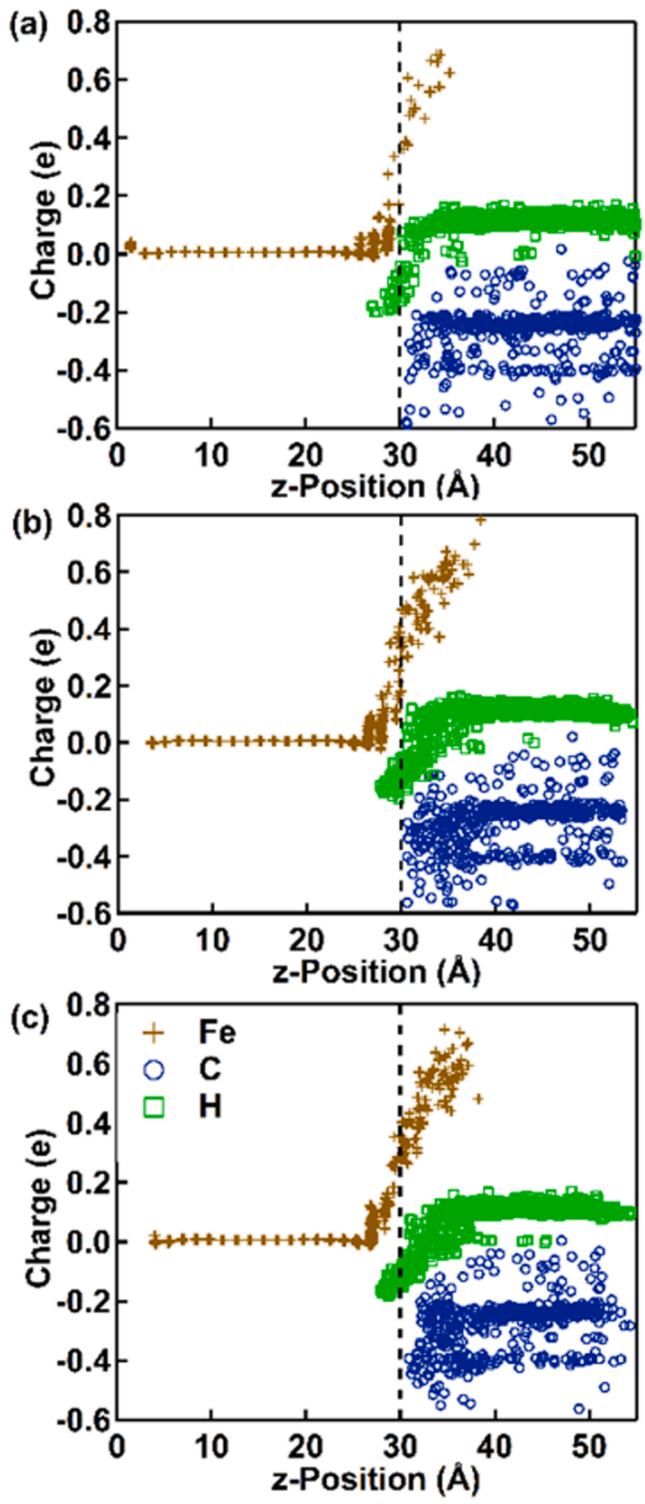

Fig. 5. Charge distribution of iron/PAO system at a temperature of 27 °C after 25 ps under (a) room pressure, (b) 140 kPa and (b) 350 kPa. Iron surface is indicated as a dashed line.

hydrogen atoms are positively charged (+0.1e) inside the PAO, while there are hydrogen atoms negatively charge near the iron-PAO interface and inside the iron slab. Those hydrogen atoms inside the iron slab have a negative charge of − 0.2e, while hydrogen atoms inside the lubricant exhibit a change less than − 0.2e. Those hydrogen atoms with a negative charge inside the lubricant form hydrogen molecules. Based on such a charge distribution, hydrogen atoms penetrated into the iron slab can be estimated in MD simulations.

The impact of temperature and pressure on the hydrogen generation is studied through estimating penetrated hydrogen atoms inside the iron slab (Fig. 6). Regardless of thermo-mechanical condition, results exhibit two stages in the hydrogen generation including a transient state and steady-state zone. There is a significant rate on the hydrogen generation at the transient stage (before 5 ps) of the chemical reactions between iron and PAO, while this rate reduces reaching to a steady-state condition mainly after 15 ps. Starting from pressure effect, the rate of hydrogen generation increases through raising the pressure, where the number of generated hydrogen at 27 °C changes from 2000 (10^{-12} mol/cm^{-2}) to 6000 (10^{-12} mol/cm^{-2}) with increasing the pressure from 100 kPa to 350 kPa. This pressure effect becomes less effective at 85 °C, where changing the pressure from 100 kPa to 350 kPa increases the number of generated hydrogen from 4500 (10^{-12} mol/cm^{-2}) to 7000 (10^{-12} mol/cm^{-2}). Although the temperature has a dramatic impact on the hydrogen generation at the atmospheric pressure, the influence of temperature becomes insignificant at higher pressures.

After analysing the hydrogen generation, decomposition of hydrocarbon is analyzed through calculating the pair distribution function for carbon (C) and hydrogen (H) bonds. Fig. 7 exhibits the effect of pressure and temperature on the decomposition process. A main peak of the pair distribution function for C-C and C-H is observed at 1.57 Å and 1.12 Å, respectively. The dominant peak for H-H bonds is found at 1.80 Å. Results show a reduction in the peak density of hydrocarbons indicating decomposition process on the iron surface, where increasing the pressure enhances the decomposition process. Increasing temperature from 27 °C and 85 °C intensifies the hydrocarbon decomposition process further. Comparing the pair distribution functions indicates that the temperature has higher impact on the decomposition process compared to the pressure.

5. Discussion

Experimental and computational results can be compared to evaluate temperature and mechanical pressures effects on the hydrogen generation in lubricated rubbing contacts. At first, one need to understand the hydrogen generation pathway from hydrocarbon lubricant as shown in Fig. 8. It has been found that nascent metal surface and shear stress catalyse the decomposition rate of the lubricant leading to higher generation of hydrogen [31,32]. Then the generated hydrogen atoms need to diffuse into the nascent steel. Therefore, the hydrogen permeation in lubricated rubbing contact has two main steps of hydrocarbon decomposition and hydrogen atom diffusion. Now, this can be analyzed from experimental and computational standpoints.

Measurement results exhibit that both temperature and mechanical pressure are effective on the hydrogen permeation in lubricated contacts (Fig. 2). In this respect, temperature is found to have a stronger impact compared to the pressure, which can be identified through comparing the current density at a pressure of 140 kPa. Although no hydrogen is detected at a pressure of 140 kPa at 27 °C, increasing the temperature to 85 °C activate the hydrogen permeation in lubricated rubbing contact. Atomic simulations demonstrated in Fig. 6 show the temperature and mechanical pressure effects on the hydrogen generation, which exhibits the same trend compared to experimental measurements. In this regard, MD simulations show the hydrogen generation at room temperature and pressure below 140 kPa, while there is no change in the current density measurements at temperature of 27 °C and pressure of 140 kPa. This can be linked to the critical load required for hydrogen permeation reported previously [31]. A minimum load is required to remove the oxide layer from the surface and forming a nascent metal surface subsequently to promote lubricant decomposition and hydrogen evolution. Increasing the contact pressure forms a larger surface area exposing more nascent surface to the lubricant, which leads to accelerating tribochemical reactions. Kohara et al. [7] reports that the hydrogen generation rate is proportional to the wear width, where there is no additive used in the

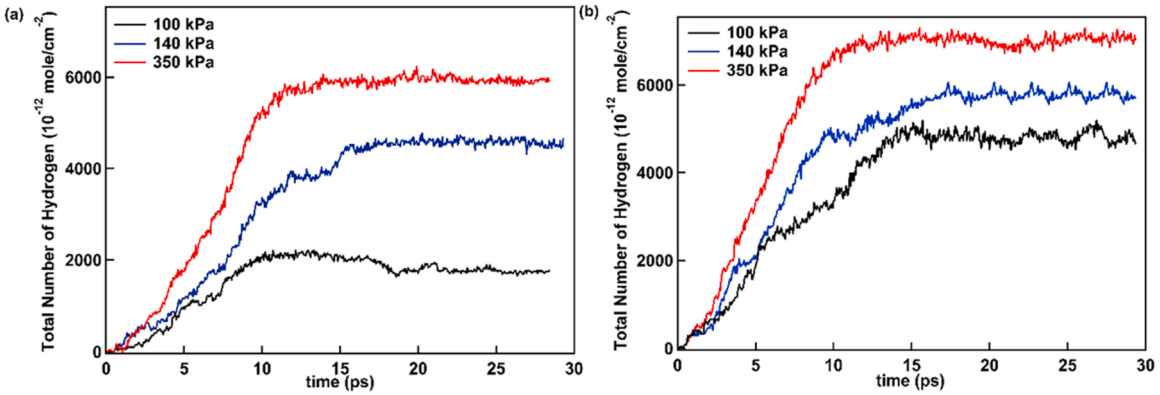

Fig. 6. Number of hydrogen atoms generated at the surface of iron as a function of time at different pressure for a temperature of (a) 27 °C and (b) 85 °C.

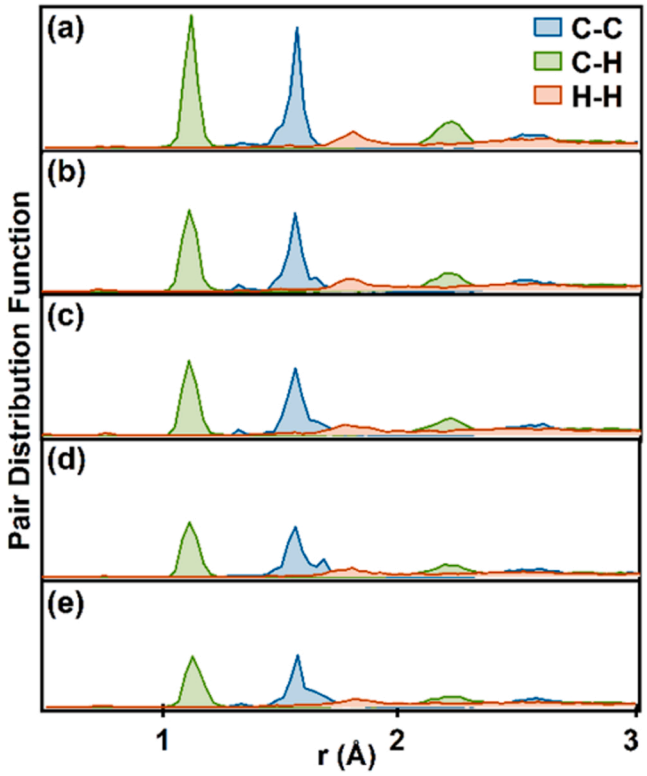

Fig. 7. Pair distribution functions of C-C, C-H and H-H bonds in hydrocarbon molecules (a) before decomposition and decomposition after 20 ps at (b) 27 °C and 100 kPa, (c) 27 °C and 350 kPa (d) 85 °C and 100 kPa and (e) 85 °C and 350 kPa.

lubricant.

The temperature effect on the hydrogen permeation can be analyzed by comparing the current density measurements (Fig. 2) and pair distribution function of the hydrocarbon decomposition demonstrated in Fig. 7. Changing the temperature from 27 °C to 85 °C enhances the decomposition process significantly, which can be seen from the pair distribution function intensity. The influence of temperature on adsorption and decomposition rate of the chemical species on the steel surface were also discussed previously [33].

The change of temperature from 27 °C to 85 °C increases the oxygen diffusion in PAO, which leads to a higher oxide scale repair with enhancing the oxidation kinetics. Although there is a higher rate of oil decomposition at 85 °C (Fig. 7) with more hydrogen generation and amorphous carbon formation, the latent time can be increased by different events. Amorphous carbon can be spread out by the slider ring and cover the emerging nascent surfaces, which reduces the penetration of hydrogen atoms into the membrane. Additionally, generation of more hydrogen along with less nascent steel surface (due to carbon contamination) may possibly create a complex layer (due to accumulation of initial hydrogen atoms forming a layer) controlling the kinetics of hydrogen diffusion into the membrane. Hence, the observed longer latent time at the higher temperature can be linked to the formation of oxide, amorphous carbon and a possible hydrogen layer formed on the nascent steel.

Both applied loads at 85°C lead to a hydrogen permeation. Considering the higher levels of dissolved O_2 at 85°C available for possible oxide repair, the rate of oxide damage should be high enough to explain the required nascent sites for hydrocarbon decomposition and hydrogen adsorption. Such damage must be of a physico-chemical nature because it can occur at the same mechanical conditions (140 kPa). Understanding the oxide effects as one possible mechanism on the hydrogen permeation in lubricated rubbing contacts needs further investigations. Induced stresses in the membrane with increasing the applied pressure can change the hydrogen permeation as well. Previous studies report a change in the hydrogen diffusivity through applying stress in metals [34,35]. Focusing on the operational factors, the presented work focuses on the thermo-mechanical analysis of lubricated rubbing contacts, while understanding the impact of stress and microstructure on the hydrogen permeation necessitates further studies.

6. Conclusions

The effect of temperature and pressure on the hydrogen generation from a lubricated rubbing contact is studied here through using a recently develop in-situ measurement approach and the reactive MD simulations. The hydrogen uptake rate as a result of PAO oil decomposition into the AISI 52100 bearing steel is measured at temperature of 27 °C to 85 °C under applied pressure of 140 kPa and 350 kPa. The reactive atomic simulations are employed to model experimental measurements. The main outcomes of the study are summarized as follow:

- Following the hydrogen generation pathway, there are two steps during the oil decomposition in rubbing contacts, hydrogen generation in atomic form and diffusion in the nascent steel. Temperature and pressure have impact on both steps in different rates.
- Both experimental measurement and computational modeling demonstrate that increasing temperature and pressure enhances the hydrogen permeation in lubricated contacts, where a stronger impact is identified from temperature. Pair distribution function in MD simulations show a higher effect of temperature on the oil decomposition process compared with pressure.
- Experimental measurements exhibit no hydrogen permeation at temperature of 27 °C and pressure of 140 kPa. Hence, a minimum load is required to remove the oxide layer from the surface and

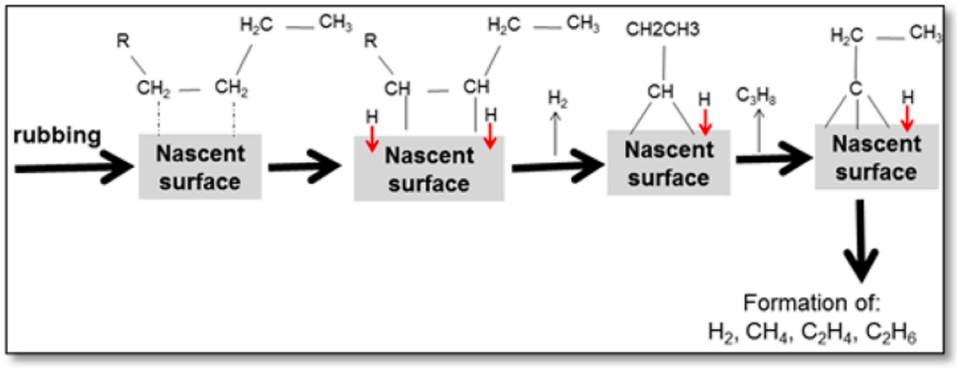

Fig. 8. Proposed reaction pathway for decomposition of hydrocarbon oil within tribocontacts [31,32].

forming a nascent metal for hydrogen permeation in lubricated rubbing contacts.

This study focuses on the incorporation of thermo-mechanical - temperature and pressure - on the hydrogen permeation in lubricated rubbing contacts. This work is carried out on pure PAO without any additives and shear stress. Understanding the influence of thermo-mechanical factors on the lubricated rubbing contact with additives and shear stresses necessitates further investigations.

Declaration of Competing Interest

The authors declare that they have no known competing financial interests or personal relationships that could have appeared to influence the work reported in this paper.

Data Availability

No data was used for the research described in the article.

Acknowledgment

The authors would like to thank Professor Anne Neville, University of Leeds, who supported this study with her guidance and encouragement.

References

[1] W. Europe, Wind energy in europe in 2018, Trends and statistics (2019).
[2] Bhadeshia H. Steels for bearings. Prog Mater Sci 2012;57:268–435.
[3] Uyama H, Yamada H, Hidaka H, Mitamura N. The effects of hydrogen on microstructural change and surface originated flaking in rolling contact fatigue. Tribology Online 2011;6:123–32.
[4] Ciruna J, Szieleit H. The effect of hydrogen on the rolling contact fatigue life of aisi 52100 and 440c steel balls. Wear 1973;24:107–18.
[5] Lu R, Shiode S, Hamada T, Tani H, Tagawa N, Koganezawa S. Effect of diamond-like carbon coating on preventing the ingress of hydrogen into bearing steel. Tribology Trans 2021;64:157–66.
[6] Lu R, Nanao H, Kobayashi K, Kubo T, Mori S. Effect of lubricant additives on tribochemical decomposition of hydrocarbon oil on nascent steel surfaces. J Jpn Pet Inst 2010;53:55–60.
[7] Kohara M, Kawamura T, Egami M. Study on mechanism of hydrogen generation from lubricants. Tribology Trans 2006;49:53–60.
[8] Ziaei S, Kokabi A, Nasr-Esfehani M. Sulfide stress corrosion cracking and hydrogen induced cracking of a216-wcc wellhead flow control valve body. Case Stud Eng Fail Anal 2013;1:223–34.
[9] Sreeraj K, Ramkumar P. Comprehensive analysis of effects of dynamic load frequency and hydrogenation to instigate white etching areas (weas) formation under severe sliding condition of bearing steel. Tribology Int 2020;144:106131.
[10] Kurten D, Khader I, Raga R, Casajus P, Winzer N, Kailer A, et al. Hydrogen assisted rolling contact fatigue due to lubricant degradation and formation of white etching areas. Eng Fail Anal 2019;99:330–42.
[11] Oezel M, Schwedt A, Janitzky T, Kelley R, Bouchet-Marquis C, Pullan L, et al. Formation of white etching areas in sae 52100 bearing steel under rolling contact fatigue–influence of diffusible hydrogen. Wear 2018;414:352–65.
[12] Evans M. White structure flaking (wsf) in wind turbine gearbox bearings: effects of 'butterflies' and white etching cracks (wecs). Mater Sci Technol 2012;28:3–22.
[13] Esfahani EA, Morina A, Han B, Nedelcu I, van Eijk MC, Neville A. Development of a novel in-situ technique for hydrogen uptake evaluation from a lubricated tribocontact. Tribology Int 2017;113:433–42.
[14] Niste VB, Tanaka H, Ratoi M, Sugimura J. Ws 2 nanoadditized lubricant for applications affected by hydrogen embrittlement. RSC Adv 2015;5:40678–87.
[15] Han B, Binns J, Nedelcu I. In situ detection of hydrogen uptake from lubricated rubbing contacts. Tribology Online 2016;11:450–4.
[16] Richardson A, Evans M-H, Wang L, Ingram M, Rowland Z, Llanos G, et al. The effect of over-based calcium sulfonate detergent additives on white etching crack (wec) formation in rolling contact fatigue tested 100cr6 steel. Tribology Int 2019;133:246–62.
[17] Ewen J, Heyes D, Dini D. Advances in nonequilibrium molecular dynamics simulations of lubricants and additives. Friction 2018;6:349–86.
[18] Liu P, Lu J, Yu H, Ren N, Lockwood FE, Wang QJ. Lubricant shear thinning behavior correlated with variation of radius of gyration via molecular dynamics simulations. J Chem Phys 2017;147:084904.
[19] Zhao X, Jin H. Investigation of hydrogen diffusion in supercritical water: a molecular dynamics simulation study. Int J Heat Mass Transf 2019;133:718–28.
[20] Minfray C, Le Mogne T, Martin J-M, Onodera T, Nara S, Takahashi S, et al. Experimental and molecular dynamics simulations of tribochemical reactions with zddp: zinc phosphate–iron oxide reaction. Tribology Trans 2008;51:589–601.
[21] Hayashi K, Tezuka K, Ozawa N, Shimazaki T, Adachi K, Kubo M. Tribochemical reaction dynamics simulation of hydrogen on a diamond-like carbon surface based on tight-binding quantum chemical molecular dynamics. J Phys Chem C 2011;115:22981–6.
[22] Nasr Esfahani M, Zare Pakzad S, Li T, Li X, Tasdemir Z, Wollschlager N, et al. Effect of native oxide on stress in silicon nanowires: Implications for nanoelectromechanical systems. ACS Appl Nano Mater 2022.
[23] Esfahani EA, Soltanahmadi S, Morina A, Han B, Nedelcu I, van Eijk MC, et al. The multiple roles of a chemical tribofilm in hydrogen uptake from lubricated rubbing contacts. Tribology Int 2020;146:106023.
[24] Svoboda J, Mori G, Prethaler A, Fischer FD. Determination of trapping parameters and the chemical diffusion coefficient from hydrogen permeation experiments. Corros Sci 2014;82:93–100.
[25] J. Kittel, F. Ropital, J. Pellier, New insights into hydrogen permeation in steels: Measurements through thick membranes., in: CORROSION 2008, OnePetro, 2008.
[26] Aryanpour M, van Duin AC, Kubicki JD. Development of a reactive force field for iron- oxyhydroxide systems, The. J Phys Chem A 2010;114:6298–307.
[27] DorMohammadi H, Pang Q, Arnaðottir L, Isgor OB. Atomistic simulation of initial stages of iron corrosion in pure´water using reactive molecular dynamics. Comput Mater Sci 2018;145:126–33.
[28] Plimpton S. Fast parallel algorithms for short-range molecular dynamics. J Comput Phys 1995;117:1–19.
[29] Colomban P, Cherifi S, Despert G. Raman identification of corrosion products on automotive galvanized steel sheets, Journal of Raman Spectroscopy: An International Journal for Original Work in all Aspects of Raman Spectroscopy. Incl High Order Process, also Brillouin Rayleigh Scatt 2008;39:881–6.
[30] Zabinski JS, McDevitt NT. Raman spectra of inorganic compounds related to solid state tribochemical studies technical report. WRIGHT LAB WRIGHT-PATTERSON AFB OH 1996.
[31] Lu R, Minami I, Nanao H, Mori S. Investigation of decomposition of hydrocarbon oil on the nascent surface of steel. Tribology Lett 2007;27:25–30.
[32] John P, Cutler J, Sanders J. Tribological behavior of a multialkylated cyclopentane oil under ultrahigh vacuum condi tions. Tribology Lett 2001;9:167–73.
[33] Shimotomai N, Nanao H, Mori S. Tribochemical reaction of benzene on nascent steel surface and effect of temperature. Tribology Online 2012;7:54–9.
[34] Park C, Kang N, Kim M, Liu S. Effect of prestrain on hydrogen diffusion and trapping in structural steel. Mater Lett 2019;235:193–6.
[35] Lu X, Díaz A, Ma J, Wang D, He J, Zhang Z, et al. The effect of plastic deformation on hydrogen diffusion in nickel Alloy 625. Scr Mater 2023;226:115210.